



A deep search for molecular gas in two massive Lyman break galaxies at z=3 and 4: vanishing CO-emission due to low metallicity?

Qinghua Tan, Emanuele Daddi, Mark T. Sargent, Georgios Magdis, Jacqueline A. Hodge, Matthieu Bethermin, Frederic Bournaud, Chris L. Carilli, Helmut Dannerbauer, Mark Dickinson, et al.

► To cite this version:

Qinghua Tan, Emanuele Daddi, Mark T. Sargent, Georgios Magdis, Jacqueline A. Hodge, et al.. A deep search for molecular gas in two massive Lyman break galaxies at z=3 and 4: vanishing CO-emission due to low metallicity?. *The Astrophysical journal letters*, 2013, 776 (2), pp.L24. 10.1088/2041-8205/776/2/L24 . cea-00998688

HAL Id: cea-00998688

<https://cea.hal.science/cea-00998688>

Submitted on 6 Jan 2021

HAL is a multi-disciplinary open access archive for the deposit and dissemination of scientific research documents, whether they are published or not. The documents may come from teaching and research institutions in France or abroad, or from public or private research centers.

L'archive ouverte pluridisciplinaire **HAL**, est destinée au dépôt et à la diffusion de documents scientifiques de niveau recherche, publiés ou non, émanant des établissements d'enseignement et de recherche français ou étrangers, des laboratoires publics ou privés.

A deep search for molecular gas in two massive Lyman break galaxies at z=3 and 4: vanishing CO-emission due to low metallicity?

Q. Tan^{1,2,3}, E. Daddi², M. Sargent², G. Magdis⁴, J. Hodge⁵, M. Béthermin², F. Bournaud², C. Carilli⁶, H. Dannerbauer⁷, M. Dickinson⁸, D. Elbaz², Y. Gao¹, G. Morrison^{9,10}, F. Owen⁶, M. Pannella², D. Riechers¹¹, and F. Walter⁵

qhtan@pmo.ac.cn

ABSTRACT

We present deep IRAM Plateau de Bure Interferometer (PdBI) observations, searching for CO-emission toward two massive, non-lensed Lyman break galaxies (LBGs) at $z = 3.216$ and 4.058 . With one low significance CO detection (3.5σ) and one sensitive upper limit, we find that the CO lines are $\gtrsim 3\text{--}4$ times weaker than expected based on the relation between IR and CO luminosities followed by similarly, massive galaxies at $z = 0\text{--}2.5$. This is consistent with a scenario in which these galaxies have low metallicity, causing an increased CO-to-H₂ conversion factor, i.e., weaker CO-emission for a given molecular (H₂) mass. The required metallicities at $z > 3$ are lower than predicted by the fundamental metallicity relation (FMR) at these redshifts, consistent with independent evidence. Unless our galaxies are atypical in this respect, detecting molecular gas in normal galaxies at $z > 3$ may thus remain challenging even with ALMA.

Subject headings: galaxies: evolution — galaxies: high-redshift — galaxies: star formation

¹Purple Mountain Observatory & Key Laboratory for Radio Astronomy, Chinese Academy of Science, Nanjing 210008, China

²CEA Saclay, DSM/Irfu/Service d'Astrophysique, Orme des Merisiers, 91191 Gif-sur-Yvette Cedex, France

³Graduate University of the Chinese Academy of Sciences, 19A Yuquan Road, Shijingshan District, Beijing 100049, China

⁴Department of Physics, University of Oxford, Keble Road, Oxford OX1 3RH, UK

⁵Max-Planck Institute for Astronomy, Königstuhl 17, 69117 Heidelberg, Germany

⁶National Radio Astronomy Observatory, P. O. Box O, Socorro, NM 87801, USA

⁷Universität Wien, Institut für Astronomie Türkenschanzstrasse, 171160 Wien, Austria

⁸National Optical Astronomical Observatory, 950 North Cherry Avenue, Tucson, AZ 85719, USA

⁹Institute for Astronomy, University of Hawaii, Honolulu, HI, 96822, USA

¹⁰Canada-France-Hawaii Telescope, Kamuela, HI, 96743, USA

¹¹Department of Astronomy, Cornell University, 220

1. Introduction

The study of cold gas, the fuel for star formation, in massive galaxies across cosmic time is crucial to understanding how galaxies have converted their gas into stars (e.g., review by Carilli & Walter 2013). Thanks to sensitivity improvements of millimeter interferometers, measurements of molecular gas have recently become feasible in normal¹ galaxies at $z \sim 0.5\text{--}2.5$ (Daddi et al. 2008, 2010; Tacconi et al. 2010, 2013; Geach et al. 2011), which lie on the star-forming main-sequence (MS). Galaxies following this relation between stellar mass and star formation rate (SFR) contribute $\sim 90\%$ to the cosmic SFR density at these redshifts (Daddi et al. 2007; Rodighiero et al. 2011; Sargent et al. 2012). It is found that these high-z star-forming galaxies are rich in molecular gas, with gas fractions ris-

Space Sciences Building, Ithaca, NY 14853, USA

¹non-starbursting

ing from $\sim 5\%$ locally to $\sim 50\%$ at $z \sim 2$ for objects with $M_\star \sim 10^{11} M_\odot$, an evolution similar to that of their specific star formation rates (sSFRs) (Magdis et al. 2012b; Tacconi et al. 2013).

However, little is known about the gas content of normal galaxies at $z \gtrsim 3$. Although CO detections have been reported in lensed Lyman break galaxies (LBGs) at $\gtrsim 3$ (Riechers et al. 2010; Livermore et al. 2012), these lenses have very low stellar masses ($M_\star \lesssim 10^9 M_\odot$) and high sSFR, and thus might not be directly comparable to more massive main-sequence galaxies at those epochs. The dependence of the CO-to-H₂ conversion factor on metallicity (e.g., Bolatto et al 2013; Carilli & Walter 2013, and references therein) may imply that CO-emission becomes weak in typical massive galaxies with low metal-enrichment at $z \gtrsim 3$ (Tacconi et al. 2008; Genzel et al. 2012; Narayanan et al. 2012).

In this Letter we present new, deeper CO observations of the $z \sim 3$ LBG M23 (for which Magdis et al. 2012a reported a $\sim 4\sigma$ CO signal), as well as of the UV-selected LBG BD29079 at $z \sim 4$ (Daddi et al. 2009). These two massive LBGs lie in the GOODS-North field. With the available optical and infrared data, we investigate their molecular gas properties and place constraints on the evolution of the molecular gas fraction, in the context of our current understanding of the metallicity-evolution of galaxies at those epochs. We assume $H_0 = 71 \text{ km s}^{-1} \text{ Mpc}^{-1}$, $\Omega_M = 0.3$, $\Omega_\Lambda = 0.7$.

2. Observations

We used the IRAM/PdBI to observe CO(4-3) emission from BD29079 and CO(3-2) from M23 (Table 1). BD29079 is in the vicinity of GN20 (separation of $\sim 16''$; Pope et al. 2005) and at the same redshift (Daddi et al. 2009). BD29079 was observed in three configurations. The pointing center of the AB-configuration observations lay $30''$ north of BD29079 (Daddi et al. 2009), while the new D- and C-configuration observations were centered on BD29079 and carried out under good 3mm weather conditions in June 2009 and January-April 2013. In total, the six antenna-equivalent on-source time for BD29079 is 13.8hr. For M23, new C-configuration observations were made in April 2013. The combination of C- and D-

configuration (Magdis et al. 2012a) observations give a total on-source time of 7.3hr. For observations made before and after 2011, correlator bandwidths are 1 GHz and 3.6 GHz (WideX), respectively. All observations were performed in dual polarization mode.

We reduced the data with the GILDAS software packages CLIC and MAPPING. After correcting for primary beam attenuation (PBA), the rms noise in a 26 km s^{-1} channel and at an angular resolution of $\sim 3.0''$ and $\sim 4.5''$ for BD29079 and M23 are 0.38 and 0.72 mJy/beam, respectively.

For BD29079, we also make use of CO(6-5) and CO(2-1) data from deep PdBI and JVLA observations of the GN20 field originally presented in Carilli et al. (2010) and Hodge et al. (2012, 2013). To avoid over-resolving of the source, the CO(2-1) data cube was tapered to a spatial resolution of $1.4''$ and binned to 26 km s^{-1} spectral resolution, with a corresponding noise of 0.21 mJy/beam. The sensitivity reached in the CO(6-5) data cube ($0.9'' \times 26 \text{ km s}^{-1}$) is 0.58 mJy/beam.

3. Results

3.1. BD29079

BD29079 is an UV-selected *B*-dropout galaxy (Figure 1) with spectroscopic redshift $z = 4.058$ (Daddi et al. 2009). CO measurements toward this galaxy were previously reported as upper limits (Carilli et al. 2011; Hodge et al. 2013). Combining our new, deep CO(4-3) data with those already published, we searched for CO-emission to deeper levels. Figure 1 shows CO spectra binned to 26 km s^{-1} at the expected frequency of CO $J=2-1$, $4-3$, and $6-5$. No line emission from the individual CO transitions was detected.

In order to maximize sensitivity, we performed a combined stack of the spectra covering all three CO transitions. The amplitude of all spectra is rescaled to the level appropriate for a template spectral line energy distribution (SLED). We consider scaling factors based on observed CO SLEDs of both sBzK galaxies and SMGs (Aravena et al. 2010; Carilli et al. 2010; Daddi et al. 2013, in preparation). In the line stack each spectrum is weighted by the inverse square of the rescaled noise. Both CO-excitation models produce no detection of the stacked line emission and lead to a comparable flux limit. We adopt an upper 3σ

TABLE 1
SUMMARY OF PdBI OBSERVATIONS

Source	R.A. (J2000)	Decl. (J2000)	Conf.	Obs. Dates	PBA	$T_{\text{int}}^{\text{a}}$ (hr)	Frequency (GHz)	Combined Beam	rms ^b (μJy)	Reference
BD29079	12:37:11.52	62:21:55.6	AB	2008 Jan-Feb	2.4	2.2	91.375	$2''.98 \times 2''.27$ P.A.=70°	29	Daddi et al. (2009)
			D	2009 Jun	1.0	7.4	91.375			This work
			C	2013 Jan-Apr	1.0	4.2	91.375			This work
M23	12:37:02.70	62:14:26.3	D	2011 May	1.0	2.5	82.059	$4''.45 \times 3''.82$ P.A.=56°	40	Magdis et al. (2012a)
			C	2013 Apr	1.0	4.7	82.059			This work

^aSix antenna-equivalent effective on-source integration time, corrected for PBA.

^bNoise per beam, averaged over full bandwidth.

CO(1-0) luminosity limit of $< 8.2 \times 10^9 \text{ K km s}^{-1} \text{ pc}^2$, derived from the flux limit of $4.1 \text{ mJy km s}^{-1}$ (1σ , assuming a line width of 300 km s^{-1}), consistent with the typical line widths measured in similarly massive high-redshift star-forming galaxies; see Daddi et al. 2010; Tacconi et al. 2010) obtained for the sBzK-excitation model². Using SMG-like CO SLEDs or those of $z \gtrsim 3$ lenses (Riechers et al. 2010; Coppin et al. 2007; Baker et al. 2004) would imply even deeper upper limits.

3.2. M23

Magdis et al. (2012a) reported CO(3-2) line emission with S/N=4 toward M23. We achieved no significant line-detection in the new observations, such that, in the combined dataset (threefold integration time increase relative to Magdis et al. 2012a), the overall significance decreases to $\sim 3.5\sigma$ (Figure 1), suggesting that the flux density reported in Magdis et al. (2012a) was boosted by noise. Based on the deeper data, we still consider the line feature in M23 as tentative and revise our estimate of its CO(3-2) luminosity to $(9.5 \pm 2.7) \times 10^9 \text{ K km s}^{-1} \text{ pc}^2$, though this may still represent an upper limit. Assuming a correction factor of $r_{31} = 0.5$ (measured in high-z normal galaxies; e.g., Dannerbauer et al. 2009; Tacconi et al. 2010), the CO(1-0) luminosity can be determined from CO(3-2) and is listed in Table 2.

²We adopt line temperature ratios of $r_{61}=0.10$, $r_{41}=0.21$, and $r_{21}=0.70$ (Aravena et al. 2010; Daddi et al. 2013, in preparation).

4. Analysis and Discussion

4.1. Physical properties

For M23, Magdis et al. (2012a) estimate SFR = $(310 \pm 110) \text{ M}_\odot \text{ yr}^{-1}$, based on radio and $250\mu\text{m}$ detections. After accounting for flux from a nearby (likely unrelated, compact, red) companion source, we revise the stellar mass estimate for M23 to $M_\star = (1.0 \pm 0.5) \times 10^{11} \text{ M}_\odot$, implying a sSFR $\sim 3.1 \text{ Gyr}^{-1}$. This value is close to the average sSFR of equally massive galaxies on the SFR- M_\star main-sequence at $z \sim 3$ (sSFR/ssSFR_{MS} ~ 1.4), suggesting that M23 is a normal galaxy rather than a starburst, notwithstanding its high SFR.

BD29079 has a stellar mass of $M_\star = (2.5 \pm 0.5) \times 10^{10} \text{ M}_\odot$, as determined by SED-fitting of the rest-frame UV-to-near-IR broad-band photometry using Bruzual & Charlot (2003) models and assuming a constant star formation history (SFH), a Chabrier (2003) IMF, and a Calzetti et al. (2000) extinction law. We infer an extinction-corrected 1500Å rest-frame luminosity corresponding to SFR of $170 \pm 40 \text{ M}_\odot \text{ yr}^{-1}$ (see Table 2). Complementary, independent constraints on the L_{IR} of BD29079 follow from its JVLA and Herschel coverage. We detect a $14\mu\text{Jy}$ -signal (4σ) in the 1.4 GHz JVLA map of Owen et al. (2013, in preparation), only slightly offset from the nominal HST position of the source. When combining this constraint with the multi-band Herschel non-detections with PACS and SPIRE, with a measurement of $0.2 \pm 0.1 \text{ mJy}$ for the 2.2mm continuum and an upper limit at 3.3mm in our PdBI data, we derive a combined estimate of $L_{\text{IR}} = (2.7 \pm 0.6) \times 10^{12} \text{ L}_\odot$, consistent within uncertainties with the extinction-corrected UV SFR

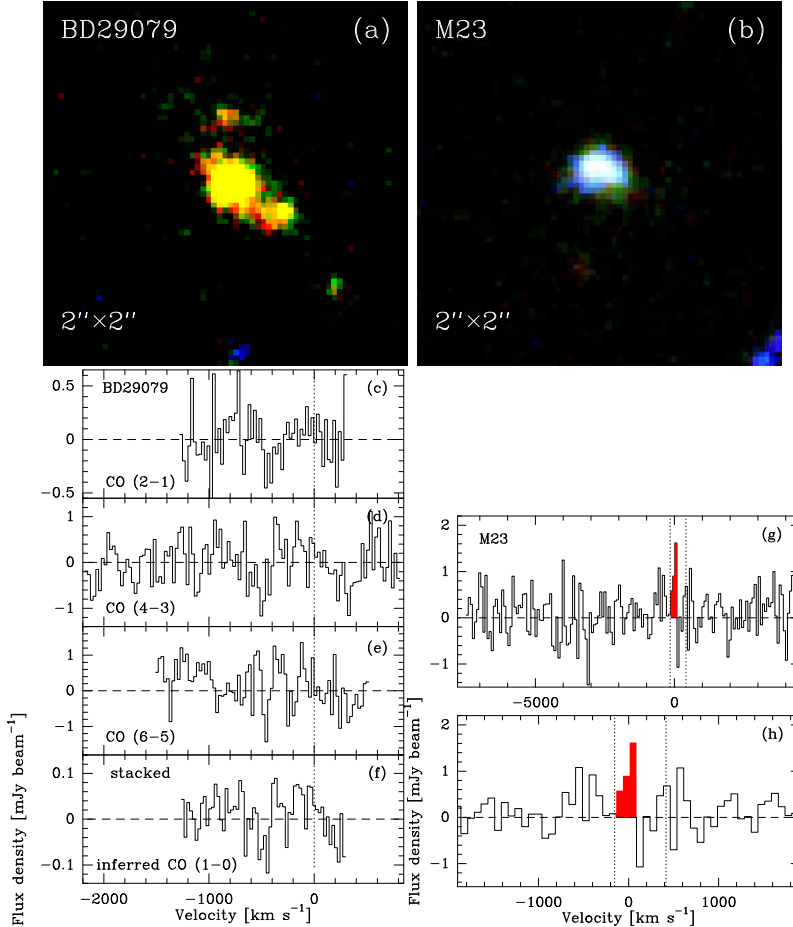


Fig. 1.— *Top:* HST+ACS color image of BD29079 (a) and M23 (b) (F435W-blue, F775W-green, and F850LP-red). The yellow color of BD29079 reflects its selection as a B-dropout. *Bottom:* CO spectra for BD29079 and M23. For BD29079, the frequency coverage of CO J=2-1(c), 4-3(d), 6-5(e), and of the stacked spectrum (f) is shown. (Spectral binning: 26 km s⁻¹; zero velocity corresponds to $z=4.058$). The stacked spectrum is produced by assuming a sBzK CO excitation model. For M23, we show the CO(3-2) spectrum with 75 km s⁻¹ spectral resolution over the full velocity range observed (h) and a zoom-in on the tentative line position (g). Red color indicates where the maximum S/N ratio is found within the velocity range given by redshift uncertainties (1σ ; dotted lines) in the optical spectroscopy (see Magdis et al. 2012a)

TABLE 2
OBSERVED AND DERIVED PROPERTIES

Source	z_{Keck}	L'_{CO} (10^{10} K km s ⁻¹ pc ²)	$M_{\text{gas}}^{\text{a}}$ ($10^{10} M_{\odot}$)	$\alpha_{\text{CO}}^{\text{b}}$ (M_{\odot} (K km s ⁻¹ pc ²) ⁻¹)	SFE (L_{\odot} (K km s ⁻¹ pc ⁻²) ⁻¹)	M_{\star}^{c} ($10^{10} M_{\odot}$)	L_{IR} ($10^{12} L_{\odot}$)	sSFR (Gyr ⁻¹)
BD29079	4.058	< 0.82 ^d	~16	>19	>330	2.5 ± 0.5	2.7 ± 0.6	10.8
M23	3.216	1.90±0.54	~18	≥9.3	≥ 160	10 ± 5	3.1 ± 1.1	3.1

^aFrom the integrated Schmidt-Kennicutt relation, M_{gas} vs. SFR (see text).

^b $\alpha_{\text{CO}} = M_{\text{gas}} / L'_{\text{CO}}$

^cStellar mass from SED fitting, assuming a Chabrier IMF

^d3 σ upper limit on CO(1-0) assuming FWHM=300 km s⁻¹.

estimate. This corresponds formally to a sSFR-excess of $\approx 2\text{--}3$ for BD29079, with respect to the characteristic value of an average main-sequence galaxy with identical mass and redshift, implying in principle a non-negligible starburst-probability for this source (e.g., Sargent et al. 2013a, henceforth S13a). While we cannot rule out the presence of a merger-induced starburst event, the fact that this galaxy was initially UV-selected, and the reasonable agreement between UV- and radio/FIR-derived SFR constraints (similar to the correspondence found for normal, massive star-forming galaxies at $z \sim 2$; see Daddi et al. 2007) disfavor this possibility.

4.2. CO luminosity

The ratio between the observables L_{IR} and L'_{CO} can be used as an indication of star formation efficiency (SFE). We find values of $\gtrsim 160$ and $> 330L_{\odot}$ ($\text{K km s}^{-1} \text{ pc}^2$) $^{-1}$ for M23 and BD29079, respectively. These are $\gtrsim 3\text{--}4$ times higher than the typical values defined by normal galaxies (Figure 2a), which display a dispersion of 0.21 dex (S13a), implying that both are $2\text{--}3\sigma$ outliers. We therefore find substantially weaker CO-emission in our two LBGs, compared to expectations based on their IR luminosities and SFRs.

We emphasize that, in term of their position in the $L_{\text{IR}} - L'_{\text{CO}}$ plane (cf. Fig. 2a), our sources and the lensed literature LBGs cB58 ($z = 2.72$), the Cosmic Eye ($z = 3.07$, Riechers et al. 2010), and the MS1358-arc ($z = 4.93$, Livermore et al. 2012) behave similarly. We caution though that the latter three are quite different sources due to their stellar masses which are ~ 2 orders of magnitude smaller than for customarily studied galaxies at $z < 4$. Lensed LBGs have also much higher sSFR values ($\sim 25\text{--}60 \text{ Gyr}^{-1}$). Even accounting for a possibly sublinear slope of the MS at $z = 3\text{--}4$, they still display excesses of $4.2\text{--}6.0$ above the MS, which would classify them as starbursting objects (Rodighiero et al. 2011). Nevertheless their CO-to-L_{IR} ratios are still factors of 2–3 smaller, even than those of the most powerful local starbursting ULIRGs (Fig.2a, dashed line). Even if the properties of these lenses are harder to interpret, they hence appear to support evidence for weak CO emission compared to lower-z sources.

4.3. Metallicity driven CO suppression

Figure 2b re-displays the same galaxies of Fig.2a, showing their CO luminosity normalized by the average $L'_{\text{CO}}(\text{SFR})$ trend of Fig.2a, and plotted as a function of redshift. Massive $z > 3$ galaxies might depart from the trend of lower-z galaxies either because they have enhanced SFR to gas mass ratios (i.e. high SFEs, implying departure from the integrated Schmidt-Kennicutt law – S-K; $\text{SFR} \propto M_{\text{gas}}^{1.2}$), or due to high CO-to-H₂ conversion factors α_{CO} caused by low metallicities. While we cannot solve the degeneracy with the available evidence, we focus on the latter effect here based on recent developments in the determination of metallicity of $z > 3$ galaxies (e.g., Maiolino et al. 2008; Sommariva et al. 2012).

To quantitatively explore the metallicity-driven suppression of CO-emission, we calculate simple models for the CO emission of galaxies based on their physical properties. We assume that normal galaxies at both $z \leq 2.5$ and $z > 3$ follow the same S-K law and have metallicity-dependent conversion factors. To a given M_{\star} and redshift, we associate SFR- and M_{gas} -values appropriate for an average main-sequence galaxy lying on the S-K law. From the M_{\star} (and SFR) we can infer the expected metallicity and thence α_{CO} and our predicted L'_{CO} (using one of three approaches discussed below), which we normalize by the average $L'_{\text{CO}}(\text{SFR})$ trend for MS galaxies from Fig.2a as for observed galaxies to display predictions in Fig.2b. A rapid decrease of metallicity, as currently suggested by high-redshift measurements, would produce outliers with weak CO-emission.

We use both the mass-metallicity ($M_{\star} - Z$) relation and the fundamental metallicity relation (FMR) relating metallicity to M_{\star} and SFR to statistically assign gas-phase metallicities (Erb et al. 2006; Sommariva et al. 2012; Zahid et al. 2013; Mannucci et al. 2010). The metallicity-dependent α_{CO} is assumed to scale as $\sim Z^{-1}$ (review by Bolatto et al. 2013; Sargent et al. 2013, in preparation, the latter study being based on the shape of the $z=0$ CO luminosity function (Keres et al. 2003)). Fig.2b shows how these simple predictions accurately describe the location of galaxies at $0 < z < 2.5$. The smoothly varying metallicity for most galaxies over $0 < z < 2.5$ causes limited variations of α_{CO} , which results

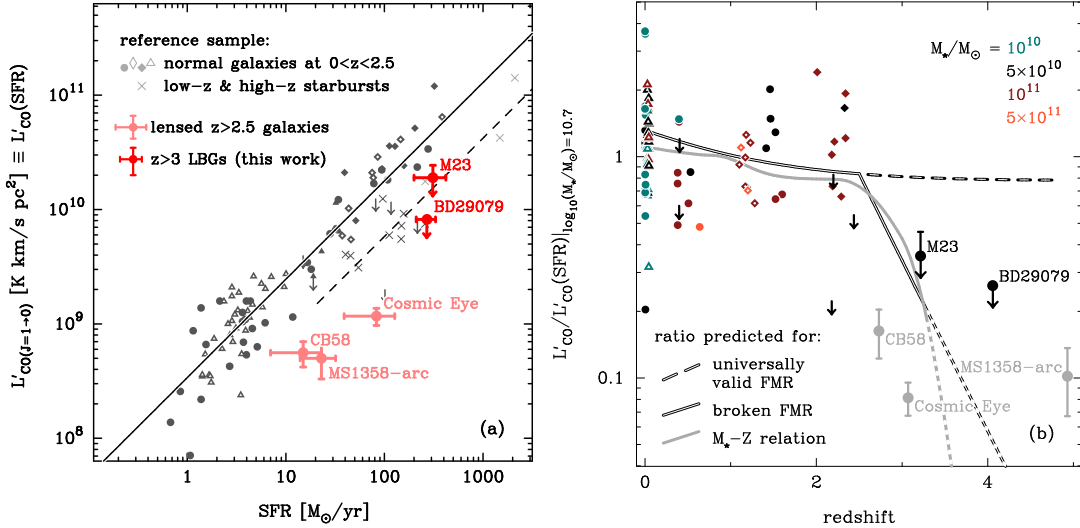


Fig. 2.— *Left:* Location of non-lensed LBGs (bright-red dots) and lensed LBGs (pale-red dots) in SFR- L'_{CO} space. Filled/open grey symbols show measurements for normal galaxies and grey crosses represent starbursts at low- and high-redshift. See Sargent et al. (2013a) for references to the literature data shown (different symbol shapes correspond to different samples). Solid and dashed lines—best-fitting relation derived for main-sequence galaxies and average offset of strong starbursts, respectively. *Right:* Redshift-evolution of the CO luminosity of galaxies, normalized by the average $L'_{\text{CO}}(\text{SFR})$ trend for MS galaxies in panel (a). Predictions are shown for the case of an universally valid FMR/broken FMR/evolving M_* – Z relation at $z \geq 3$ (dashed/solid/grey lines; the $z > 3.5$ extrapolations are observationally-unconstrained). All measurements for normal galaxies (colored points) and predictions have been normalized to a common mass scale of $M_* = 5 \times 10^{10} M_\odot$ based on the expected mass dependence of $L'_{\text{CO}}/L'_{\text{CO}}(\text{SFR}) \propto M_*^{0.3}$. Data points are colored depending on which reference color was closest in stellar mass. No mass-dependent scaling was applied to the lensed, possibly starburst-like $z > 3$ sources.

in a tight L'_{CO} –SFR relation, and thus only weak scatter in both Fig. 2 panels. However, the systematic decrease of α_{CO} with increasing M_* produces small mass-dependent drifts that we correct in both data and models (see caption of Fig. 2).

Figure 2b shows tracks for the case of an FMR that remains constant at all redshift, for an FMR that breaks at $z=2.5$, and for a $M_* - Z$ relation with accelerated evolution at $z > 2.5$. Evidence for metallicity evolution at $z > 2.5$ comes from Mannucci et al. (2010) and Sommariva et al. (2012). For the scenario with a broken FMR, we interpolate linearly with redshift the metallicity drop of 0.6 dex reported in Mannucci et al. (2010) between $z=2.5$ and $z=3.3$ and continue this trend beyond $z=3.3$ to estimate high-z evolution (but see Hunt et al. 2012 for a non-evolutionary interpretation of the low-metallicity readings at high-redshifts). For the case of an evolving $M_* - Z$ relation, a similar linear interpolation/extrapolation is applied between $z=2.2$ and $z=3$ based on the $M_* - Z$ relations of Sommariva et al. (2012) and Zahid et al. (2013). A distinct difference among these predic-

tions is the rapid decrease of the $L'_{\text{CO}}/L'_{\text{CO}}(\text{SFR})$ ratio at high- z in the case of fast metallicity evolution at $z > 2.5$. For the case of an universally valid FMR, the evolution of $L'_{\text{CO}}/L'_{\text{CO}}(\text{SFR})$ is not overly strong and almost vanishes at fixed M_* . The scatter of the reference $z < 2.5$ sample around the average predicted trend is 0.24 dex. M23 starts to deviate from the constant FMR track, agreeing better with the prediction assuming a rapid decline in metallicity at $z \sim 3$. BD29079 displays an offset of $> 2\sigma$ relative to the scenario of an universally-valid FMR.

4.4. The CO to H₂ conversion factor in a regime of evolving metallicity

Metallicity evolution with redshift would affect, as discussed, the CO-to-H₂ conversion factor, making it challenging to infer the H₂-content from CO-measurements. The two massive LBGs studied here exemplify this: under the aforementioned, different plausible scenarios, α_{CO} could range over 4–12 M_\odot ($\text{K km s}^{-1} \text{pc}^2$) $^{-1}$ for M23 and 7–63 for BD29079. Inferring α_{CO} at $z \gtrsim 3$ is even much harder than at $z \sim 1.5 - 2$. An overall better,

average estimate of molecular gas mass could arguably be derived from the SFR itself, via the integrated S-K relation rather than from CO-emission (though we caution that no guarantee exists that the S-K still holds unchanged at $z > 3$). Adopting the well-established relation between M_{gas} and SFR for normal galaxies as in S13a, we infer molecular gas masses $M_{\text{gas}} \sim 1.6 \times 10^{11} M_{\odot}$ and $M_{\text{gas}} \sim 1.8 \times 10^{11} M_{\odot}$ for BD29079 and M23, respectively. With $M_{\text{gas}} = \alpha_{\text{CO}} L'_{\text{CO}}$, the corresponding α_{CO} would be > 19 and $\gtrsim 9.3$ for BD29079 and M23.

4.5. The evolution of molecular gas fraction

Recent studies reported a trend for increasing molecular gas fractions ($f_{\text{gas}} = M_{\text{gas}} / [M_{\text{gas}} + M_{\star}]$) with redshift up to $z \sim 2.5$ (Daddi et al. 2010; Geach et al. 2011; Magdis et al. 2012a; Tacconi et al. 2013; Saintonge et al. 2013), in good agreement with the redshift evolution of sSFR (Magdis et al. 2012b), suggesting that the peak epoch of cosmic star formation ($z \sim 2$) corresponds to an epoch when typical massive galaxies were dominated by molecular gas. Some works have highlighted the impact of the assumed SFH and of nebular emission on SED-fitting and consequently on the measured sSFR-evolution beyond $z \sim 2$ (de Barros et al. 2013; González et al. 2013), in light of the disagreement between the observed sSFR plateau and current theoretical predictions (Neistein & Dekel 2008; Weinmann et al. 2011). Given the tight correlation between SFR and molecular gas content, the study of gas fractions in galaxies at $z > 3$ might be useful to investigate the putative sSFR-plateau at $z \sim 2-8$.

Figure 3 shows the evolution of M_{gas}/M_{\star} for normal galaxies with $\text{sSFR}/\text{sSFR}_{\text{MS}} = 1$ and $M_{\star} = 5 \times 10^{10} M_{\odot}$ out to $z \sim 4$. Gas fractions of galaxies with $M_{\star} \neq 5 \times 10^{10} M_{\odot}$ were rescaled based on the observed trends $M_{\text{gas}}/M_{\star} \propto (\text{sSFR}/\text{sSFR}_{\text{MS}})^{0.9}$ and $M_{\text{gas}}/M_{\star} \propto M_{\star}^{-0.5}$ (Magdis et al. 2012b). For the case of an universally valid FMR, we infer M_{gas}/M_{\star} of $\lesssim 0.72$ and < 0.65 for M23 and BD29079, which in both cases is lower than expected based on the observed sSFR-evolution, i.e., an increase with $(1+z)^{2.8}$ to $z \sim 2.5$, followed by a plateau or a slow rise at even higher redshifts. Larger gas fractions are obviously recov-

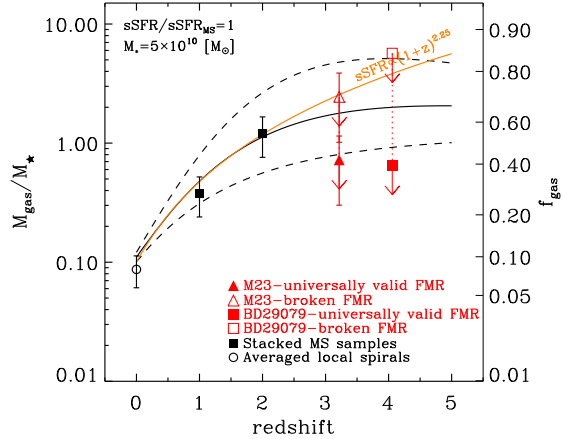


Fig. 3.— Redshift-evolution of M_{gas}/M_{\star} and the molecular gas fraction of normal galaxies with $\text{sSFR}/\text{sSFR}_{\text{MS}} = 1$ and $M_{\star} = 5 \times 10^{10} M_{\odot}$. We compare the LBGs of this study to the $z = 0$ sample of Leroy et al. (2008), and stacked samples of $z \sim 1$ and $z \sim 2$ normal galaxies from Magdis et al. (2012b). Gas fraction estimates for M23 and BD29079 derived assuming an universally valid (broken) FMR at $z \geq 3$ are marked with solid (open) red symbols. Black-solid line – evolution of M_{gas}/M_{\star} at $M_{\star} = 5 \times 10^{10} M_{\odot}$, predicted based on the observed sSFR-evolution (S13a; dashed line – $\pm 1\sigma$ uncertainties). The orange line traces the evolution predicted by the model of Davé et al. (2012).

ered if, as in the previous sections, we allow for rapidly declining metallicities. If we assume strong metallicity-evolution at $z > 2.5$, the gas fractions of M23 and BD29079 appear to agree with the measured sSFR-evolution, and also with some theoretical predictions, e.g. for the case of a continuously increasing $\text{sSFR} \propto (1+z)^{2.25}$, as expected for accretion of pristine gas from the intergalactic medium (Davé et al. 2012). Given the low significance of our CO-detections and the large systematic uncertainties, our results can only delimit a range for the evolution of gas fractions at $z \sim 3-4$. Additional, direct metallicity estimates for high redshift galaxies would be highly beneficial for further exploration of the evolution of gas fractions. A larger sample of normal galaxies with CO-detections at $z > 3$ is also clearly needed to reach firm conclusions.

5. Conclusions

We presented evidence that the CO-emission from two $z \gtrsim 3$ massive LBG galaxies is weaker than expected based on the tight correlation between IR and CO luminosities satisfied by similar $z \leq 2.5$ objects. A plausible explanation is

that $z > 3$ normal galaxies are weak in CO due to rapid metallicity-evolution at high redshift. As a result, the evolution of molecular gas fractions beyond $z \sim 3$ is fairly uncertain due to the large uncertainties on metallicity-estimates and the shape of the relation between CO-to-H₂ conversion factor and metallicity. Also, the exact normalization and dispersion of the main-sequence is not well constrained at these redshifts, and their attenuation properties might have evolved, thus making it even harder to distinguish normal disk-like galaxies from merger-powered sources. Our observations (similarly to results of Ouchi et al. 2013) in any case start to point to the difficulty of detecting gas cooling emission lines from normal galaxies at $z > 3$. This might remain challenging even with the unprecedented sensitivity of ALMA if metallicities indeed decrease rapidly for typical massive galaxies at these high redshifts.

This work was based on observations carried out with the IRAM PdBI, supported by INSU/CNRS (France), MPG (Germany), and IGN (Spain). We thank C. Feruglio and M. Krips for help during observations/data reduction, and the anonymous referee for valuable comments. QT, ED, MTS and MB acknowledge funding from ERC-StG grant UPGAL 240039 and ANR-08-JCJC-0008.

REFERENCES

- Aravena, M., Carilli, C., Daddi, E., et al. 2010, ApJ, 718, 177
- Baker, A. J., Tacconi, L. J., Genzel, R., et al. 2004, ApJ, 604, 125
- Bolatto, A. D., Wolfire, M., Leroy, A. K. 2013, ARA&A, 51, 207
- Bruzual, G., & Charlot, S. 2003, MNRAS, 344, 1000
- Calzetti, D., Armus, L., Bohlin, R. C., et al. 2000, ApJ, 533, 682
- Carilli, C. L., Daddi, E., Riechers, D., et al. 2010, ApJ, 714, 1407
- Carilli, C. L., Hodge, J., Walter, F., et al. 2011, ApJ, 739, L33
- Carilli, C. L., & Walter, F. 2013, ARA&A, 51, 105
- Chabrier, G. 2003, PASP, 115, 763
- Coppin, K. E. K., Swinbank, A. M., Neri, R., et al. 2007, ApJ, 665, 936
- Daddi, E., Dickinson, M., Morrison, G., et al. 2007, ApJ, 670, 156
- Daddi, E., et al. Dannerbauer, H., Elbaz, D., 2008, ApJ, 673, 21
- Daddi, E., Dannerbauer, H., Stern, D., et al. 2009, ApJ, 694, 1517
- Daddi, E., Bournaud, F., Walter, F., et al. 2010, ApJ, 713, 686
- Dannerbauer, H., Daddi, E., Riechers, D. A., et al. 2009, ApJ, 698, 178
- Davé, R., Finlator, K., Oppenheimer, B. D. 2012, MNRAS, 421, 98
- de Barros, S., et al. 2013, arXiv: 1207.3663
- Erb, D. K., Shapley, A. E., Pettini, M., et al. 2006, ApJ, 644, 813
- Geach, J. E., Smail, I., Moran, S. M., et al. 2011, ApJ, 730, 19
- Genzel, R., Tacconi, L. J., Combes, F., et al. 2012, ApJ, 746, 69
- González, V., et al. 2013, arXiv: 1208.4362
- Hodge, J. A., Carilli, C. L., Walter, F., et al. 2012, ApJ, 760, 11
- Hodge, J. A., et al. 2013, arXiv: 1307.4763
- Hunt L., Magrini, L., Galli, D., et al., 2012, MNRAS, 427, 906
- Keres, D., Yun, M. S., Young, J. S. 2003, ApJ, 582, 659
- Leroy, A. K., Walter, F., Brinks, E., et al. 2008, AJ, 136, 2782
- Livermore, R. C., Swinbank, A. M., Smail, I., et al. 2012, ApJ, 758, L35
- Magdis, G. E., Daddi, E., Sargent, M., et al. 2012a, ApJ, 758, L9
- Magdis, G. E., Daddi, E., Béthermin, M., et al. 2012b, ApJ, 760, 6
- Maiolino, R., Nagao, T., Grazian, A., et al. 2008, A&A, 488, 463
- Mannucci, F., Cresci, G., Maiolino, R., et al. 2010, MNRAS, 408, 2115
- Narayanan, D., Krumholz, M. R., Ostriker, E. C., et al. 2012, MNRAS, 421, 3127
- Neistein, E., & Dekel, A. 2008, MNRAS, 383, 615
- Ouchi, M., Ellis, R., ONO, Y., et al. 2013, arXiv: 1306.3572
- Pope, A., Borys, C., Scott, D., et al. 2005, MNRAS, 358, 149
- Riechers, D. A., Carilli, C. L., Walter, F., et al. 2010, ApJ, 724, L153
- Rodighiero, G., Daddi, E., Baronchelli, I., et al. 2011, ApJ, 739, 40
- Saintonge, A., Lutz, D., Genzel, R., et al. 2013, arXiv: 1309.3281
- Sargent, M. T., Béthermin, M., Daddi, E., et al. 2012, ApJ, 747, L31
- Sargent, M. T., Daddi, E., Béthermin, M., et al. 2013, arXiv: 1303.4392 (S13a)

- Sommariva, V., Mannucci, F., Cresci, G., et al. 2012, A&A, 539, 136
- Tacconi, L. J., Genzel, R., Smail, I., et al. 2008, ApJ, 680, 246
- Tacconi, L. J., Genzel, R., Neri, R., et al. 2010, Nature, 463, 781
- Tacconi, L. J., Neri, R., Genzel, R., et al. 2013, ApJ, 768, 74
- Weinmann, S. M., Neistein, E., Dekel, A., et al. 2011, MNRAS, 417, 2737
- Zahid, H. J., Geller, M., Kewley, L., et al. 2013, ApJ, 771, 19